Urban Climate 56 (2024) 102079

Contents lists available at ScienceDirect

Urban Climate

journal homepage: www.elsevier.com/locate/uclim

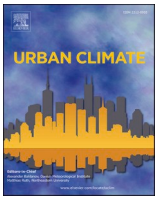

Evaluation of the intensity of urban heat islands during heat waves using local climate zones in the semi-arid, continental climate of Tehran

Gholamreza Roshan [a,*], Saleh Arekhi [a], Zainab Bayganeh [a], Shady Attia [b]

[a] Department of Geography, Golestan University, Gorgan, Iran
[b] Sustainable Buildings Design Lab, Dept. UEE, Applied Sciences, Université de Liège, Belgium

ARTICLE INFO

Keywords:
Climate mitigation
Heat island severity
Heatwave warning system
Land use
Urban green space

ABSTRACT

Increasing land surface temperature (LST) and urban heat island intensity (UHII) have been reported to be closely associated with a large number of environmental issues. Understanding LST and UHII rise in cities during heatwaves is crucial for implementing mitigation measures. This paper aims to explain these variations in response to LST and UHII during a heat wave in the metropolis of Tehran in Iran. 13 heat waves were selected and evaluated during the years 2000 to 2020. The average LST was 3.34 °C higher at the same time as the heat wave event compared to the period without the wave. Despite the increase in LST during the heat wave occurrence, UHII experienced lower values compared to the time without the wave. The outputs in this regard show that the average UHII value for the period without a heat wave is 5.11 °C, while during the heat wave, its rate is 3.62 °C. The maximum intensity of the heat island for both periods before and at the same time as the heat wave is related to man-made compact midrise buildings and heavy industry. Extra-local factors during heat waves can lead to diminish land use diversity and vegetation density's effectiveness in reducing UHII.

1. Introduction

The relationship between urbanization, climate change and microclimate in the built environment is complex (Makvandi et al., 2019; Yang et al., 2023). With the proliferation of satellite map datasets with historical observations of land surface temperature and an abundance of weather datasets from weather stations around cities, there is an opportunity to contribute further to the understanding of this complex relationship (Good et al., 2017), especially during heat waves (Gogoi et al., 2019). Remoting sensing can sometimes stay superficial and two-dimensional, failing to characterize the spatial and temporal variations of the urban thermal layer, especially in cities. Therefore, coupling the satellite maps with historical observations of land surface temperature (LST), thermal bands, red bands near-infrared bands with ambient air temperature from weather files can improve the characterization of the urban thermal layer and accurately articulate its uniformity.

In many large global cities, the relationship of surface urban heat islands with air temperature and precipitation is relatively stable, with positive correlations during the day and negative correlations at night, and shows no obvious differences in macro-climatic conditions and urban size (Li et al., 2020). However, on the micro-scale, the urban thermal layer remains not uniform and varies

* Corresponding author.
E-mail address: ghr.roshan@gu.ac.ir (G. Roshan).

https://doi.org/10.1016/j.uclim.2024.102079
Received 7 April 2024; Received in revised form 19 June 2024; Accepted 23 July 2024

spatially depending on the urban morphology, surface materials and vegetation (Lai et al., 2019). A closer characterization is needed on the microscale to identify the hotspots on the urban scale, especially in cities with large populations (Schwarz et al., 2012).

Therefore, the current research aims to analyze the relationship between heat waves and UHIs in the metropolis of Tehran and to evaluate the role of different land uses in the UHII during the years 2000 to 2020. Tehran city experiences heat waves in some periods due to exposure to the influence of the Azores and the hot and dry air of the African and Arabian deserts (Darand and Halabian, 2013; Nasiri, 2016; Barati et al., 2021). The following research questions are guiding the research investigation toward a better understanding of the complex relationship between urbanization and microclimate during heat waves (Good et al., 2017). The research answers the following questions:

- What is the frequency occurrence and intensity of heat waves in Tehran between 2000 and 2020?
- What are the spatial-temporal patterns of urban heat islands in Tehran before and after heat waves?
- What is the effect of local climate zones and vegetation on the urban heat island intensity patterns?

Understanding the characteristics of heat waves in this city and their effect on UHII is an important issue that can help planning in different sectors such as water resources, agriculture and the environment and provide the necessary awareness, recommendations and solutions. The results are key to understanding the local climate and the cities' hot spots during heat waves. More importantly, results can be presented to city managers, landscape designers, gardeners and climate department officials in cities for the unexpected events in Tehran and cities in the same climatic class of the semi-arid, continental climate. As can be seen in Fig. 1, there are major cities with similar climates in other regions around the world. Therefore, our study will be useful to improve the understanding of the impact of heat waves on the urban heat island effect intensity (UHII) and allow the deepening of the understanding of this complex relationship globally and better manage it (Daniel et al., 2018).

Investigating the relationship between heat waves and UHIs in recent years has often attracted the attention of researchers around the world (Cui et al., 2023; Cheval et al., 2024; Dezső et al., 2024). However, in Iran, these two phenomena have often been studied separately, and in limited studies (Ghobadi et al., 2018; Keikhosravi, 2019; Firozjaei et al., 2020), the effect of heat waves on the changes in the UHII pattern has been studied. Therefore, the current study considers the changes in the UHII for the period before and during the heat wave event. It will be evaluated for 13 study cases for the city of Tehran.

In this research, the behavior of different local climate zones in the spatial pattern of UHII will be investigated. The research methodology followed four key steps. First, the threshold of heat wave occurrence and an analysis of their frequency, intensity and continuity for the city of Tehran during the years 2000 to 2020. In the next step, the determination of 13 selected heat waves and monitoring of spatial-temporal LST patterns before and simultaneously with the occurrence of the wave heat. In the third step, determine the intensity pattern of the heat island and compare it before and simultaneously with the consequence of the heat wave. In the final stages, evaluate the role of local climate zones and changes in the Normalized difference vegetation index (NDVI) in the formation of different patterns of UHII throughout Tehran.

2. Literature review

A heat wave is defined as an unusual and exceptional continuation of hot weather that can create a crisis for humans and the environment (Nobert and Pelling, 2017; Cuerdo-Vilches et al., 2023) and reducing the consequences of this risk depends on identifying the atmospheric systems that create and predicting the time and place of their occurrence (Alghamdi and Harrington, 2016; Fonseca-Rodríguez et al., 2023). Cities, in most cases, experience special climatic conditions called urban climate. Urban climate through the

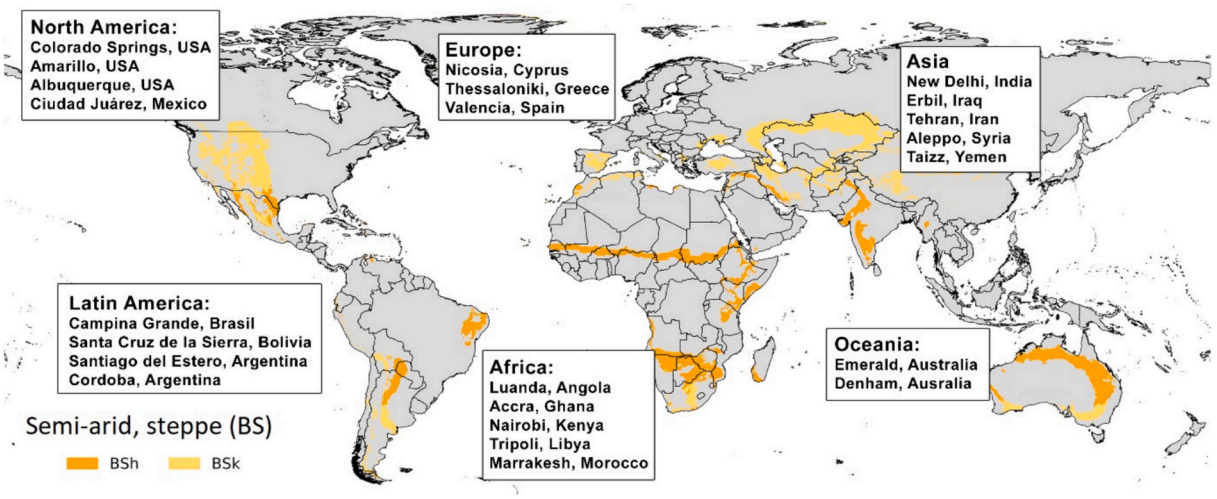

Fig. 1. Cities with hot semi-arid (steppe) climate (BSh) worldwide (Peel et al., 2007).

difference in the climatic variables of the city (temperature, humidity, wind, precipitation) from the less dense surrounding areas is identified (Kuttler, 2008).

The land surface temperature is one of the key parameters in the physical, chemical and biological control of earth processes. It is considered an important factor in the study of urban climate. Khandelwal et al. (2017); Masson et al. (2020). The stagnant atmospheric conditions resulting from heat waves trap pollutants in urban areas. The addition of severe stress of toxic pollutants to the dangerous stress of the existing hot air creates an environmental problem on a large scale (Almusaed, 2011: 139; Yilmaz et al., 2023; Tsao et al., 2023).

Researchers believe that during recent years, climate change and global warming have led to an increase in the frequency and continuity of heat waves in different parts of the world. Therefore, the continuous increase in the temperature of the city as a UHI on the one hand and the sudden occurrence of heat waves as one of the important climate hazards on the other hand, have caused the concern of urban management policymakers (Mika et al., 2018; Yang et al., 2020; Ullah et al., 2023; Singh and Mall, 2023; Caldeira et al., 2023). Because the occurrence of these two phenomena can intensify the heat of the cities, especially in the big cities, and as a result, it will cause much environmental damage.

According to the explanations provided and considering the adverse environmental consequences and the consequences of extreme climatic events such as heat waves, the need for research in this field becomes more apparent. On the other hand, one of the environmental hazards and ecological crises that the world is facing today is the phenomenon of land use change (Yu and Zhou, 2018; Ma et al., 2018; Wang and Wang, 2022). Urbanization has changed the types of land cover in urban areas, which leads to the formation of distinct climates compared to the surrounding areas. Land use changes affect a wide range of environmental characteristics of cities, including their atmospheric pattern and air quality (Kılkış, 2022; Pande et al., 2023).

Timely and accurate detection of these types of changes is the basis of a better understanding of the relationships and interactions between humans and natural phenomena, and as a result, provides better management and more appropriate use of natural resources. The process of indiscriminate construction and reduction of green spaces as urban lungs leads to negative changes in the microclimate of cities. The type of land use plays a very important role in the LST of cities and is influential in the formation of the UHI (Chen et al., 2022; Yuan et al., 2023; Najah et al., 2023).

Therefore, this study aims to bridge this knowledge gap by charcterisation of the UHII during heat waves in the diverse urban morphology of Tehran. The current study considers the changes in the UHII for the period before and at the same time as the heat wave event.

3. Study region

The Tehran study region is located in the northern portion of the central Iranian plateau (35°07′ N; 51°24′ E) and covers an area of 18,909 km^2. Over the past few decades, Tehran's population has been steadily growing and is currently estimated at around 8.3 million (Dadashpoor, 2017). The climate in Tehran is semi-arid with a continental character, but it also exhibits a Mediterranean-type precipitation pattern (Koppen¨climate classification: BSk).

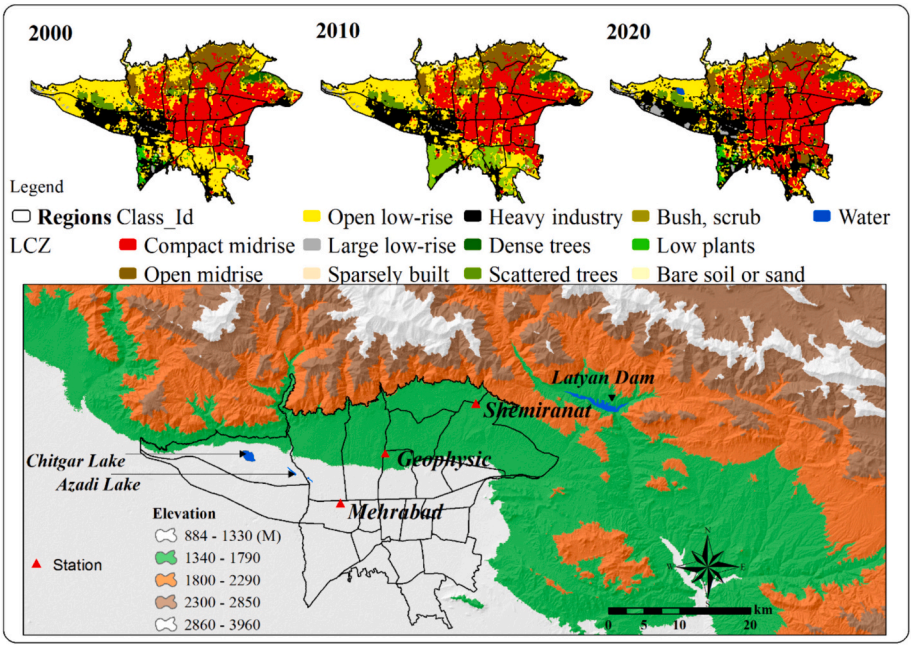

Fig. 2. The study region illustrates the changes in land use over time and the main weather stations utilized in this research.

The city's geographic location, particularly its proximity to the Alborz Mountains in the north, greatly influences its climate by causing cold and subsiding airflow. Summers in Tehran are generally hot and dry, with an average temperature of 28.8 °C. Spring and autumn are mild and relatively dry, with mean temperatures of 22.6 °C and 11.9 °C, respectively. Winters are cold and wet, with an average temperature of 6.8 °C (Roshan et al., 2010; Ghanghermeh et al., 2013, 2019).

4. Data and methodology

Two types of data are used in the present study. The first category includes air temperature (AT) data that is measured at the weather station level, and the other is data related to satellite images. The land surface temperature can be mentioned among the data related to satellite images. The data related to AT includes the average daily temperature values of meteorological stations in Tehran (Mehrabad, Geophysics and Shemiranat stations) (Fig. 2) for the period 1990 to 2020, which was prepared by the Islamic Republic of Iran Meteorological Organization (IRIMO).

At first, based on the data from three meteorological stations, a total average was extracted, and other works were done on this time series. In this study, heat wave event periods were identified using mean daily air temperature data. In the current research, although our main focus is only on the time series of 2000 to 2020, in order to determine the appropriate threshold of heat wave occurrence, the length of the study period was extended to 30 years (1990 to 2020). The threshold of heat wave occurrence can be identified based on a standard statistical period. In general, there is no uniform and comprehensive method for identifying heat waves. At the same time, one of these methods is using the 95th percentile of the AT component (Anderson and Bell, 2011; Xu et al., 2016; Roshan et al., 2018; Sharafkhani et al., 2020).

Therefore, based on the 95th percentile index of the mean daily AT component, the threshold for the occurrence of a heat wave for the city of Tehran was determined as 32.32 °C. On the other hand, it is necessary to explain that the AT threshold is not the only criterion to determine the heat wave. Rather, time continuity is also considered as a measure of heat wave occurrence. In various studies, this duration is considered to be at least 3, 5 or 7 days (Huynen et al., 2001; Kornus et al., 2023). In the current research, a period in which the mean daily AT threshold exceeds the 95th percentile for at least three continuous days is known as a heat wave. The coldest day experienced in the 2 weeks before the wave event is introduced as the No heat wave period (Maleki Meresht et al., 2021; Maleki Rashti et al., 2022).

4.1. Extraction of LST data from MODIS sensor and calculation of UHII

The MODIS sensor is installed on two AQUA and TERRA satellites and has been covering the earth since 2000. The MODIS sensor has 36 spectral bands in the visible, reflective infrared and thermal infrared spectral ranges. Meanwhile, 20 bands in the reflective range and 16 bands in the thermal range take images. From a spatial point of view, the measuring bands of MODIS produce images with an accuracy of 250, 500 and 1000 m and provide the possibility of monitoring land changes on a daily basis. In this research, MODIS thermal bands with a spatial resolution of 1 km have been used.

MODIS images are captured for the entire earth once every 2 days, with the satellite orbit taking 99 min. All 36 MODIS bands are used for daytime imaging, and bands 20–36 (MODIS thermal bands) bands are used for nighttime imaging. Normally, the overpass of Terra satellite's sensor for Iran is between 10:30 and 11:30 am (local time) in the morning and for the evening at about 22:30 pm (Roshan et al., 2022).

Nighttime temperature data are more accurate compared to daytime data because there is no effect of daily solar radiation in them, and it is possible to estimate temperature with higher accuracy. In this regard, nighttime thermal data allows more accurate monitoring of the urban heat island (Reisi et al., 2019; Siddiqui et al., 2021). Therefore, in the present study, night LST has been used in order to identify the temporal-spatial patterns of UHII. It is worth mentioning that for each period of heat wave occurrence with different durations, an average LST of that period has been prepared. For the period without a heat wave, the LST corresponds to the coldest day that was experienced at most 2 weeks before the heat wave period. The specifications for each of the images were obtained from the Google Earth Engine system, related to the Terra satellite MODIS sensor.

In general, human activities, land uses and population of the urban environment are all factors that increase the LST of the city compared to its surrounding environment. This LST difference between the urban and its surroundings is known as the UHI (Cai et al., 2023; Foissard et al., 2019). By using satellite images in remote sensing, it is possible to identify and monitor its changes. However, UHI detection techniques may have differences. In this study, two methods have been used to study the UHII. First, the temperature difference between the LST of the over urban area ($\overline{\mathrm{LST}}_{Urban}$) compared to the overall mean LST of the suburbs (rural) $\overline{\mathrm{LST}}_{Rural}$ is a criterion for determining the UHII, which is calculated as follows (Eq. 1):

$$\mathrm{UHII} = \overline{LST}_{Urban} - \overline{\mathrm{LST}}_{Rural} \tag{1}$$

The mean LST of all the cells inside the urban was used, and the suburb area (rural) was considered at a distance of less than 3 km around it to determine the LST of the urban area. In order to determine the LST of the suburban area, similar to the urban area, the LST of all the cells inside this area was calculated, and its average was used to determine the UHII.

But in the second method, for mapping, the LST difference between the LST of each pixel (LST_{P_i}) compared to the overall average LST of the countryside (village) $\overline{\mathrm{LST}}_{Rural}$ was calculated. In the second method, an output is extracted for each pixel, based on which mapping is also done. This method is also introduced with the abbreviation PUHII (Eq. 2):

$$PUHII = LST_{P_i} - \overline{LST}_{Rural} \quad (2)$$

4.2. Production of the normalized difference vegetation index map

The normalized difference vegetation index (NDVI) is a widely used metric for quantifying the health and density of vegetation using sensor data. It is calculated from spectrometric data at two specific bands: red and near-infrared. The spectrometric data is usually sourced from remote sensors, such as satellites.

In this study, Landsat satellites 7 and 8 from 2000 to 2020 are used to collect thermal bands, red bands (RED) and near-infrared bands (NIR). For this purpose, we considered days with 10% or less cloud cover. The LST was estimated using pre-processed spectral bands in an 'Earth Engine' environment, as explained in the previous section, and then NDVI was estimated using the equation below (Nakano et al., 2023):

$$NDVI = \frac{NIR - RED}{NIR + RED} \quad (3)$$

In Table 1, the details of Urban vegetation classes and NDVI value are provided (Akbar et al., 2019):

4.3. Production of local climate zones map

Physical development and climate change contribute to the Urban Heat Island (UHI) effect and significant temperature differences between cities and their surrounding areas. However, the urban thermal layer is not uniform and varies spatially and temporally. The variability in the urban thermal layer, which can be measured using near-surface air cover, depends on land use/cover types and human activities. Consequently, the diversity and intensity of human activities in different parts of the urban environment create varying microclimates.

Classifying satellite images and producing thematic maps, including land use maps and distinguishing urban areas from more open or barren lands, pose challenges and may contain subtle errors. Nevertheless, in recent years, a widely-used method called 'Local Climate Zone' (LCZ) classification has been developed to address some of these challenges (e.g., Daramola and Balogun, 2019; He et al., 2019; Kotharkar and Bagade, 2018; Roshan et al., 2021). The LCZ classification strategy defines and establishes standardized urban classification using satellite images. It separates different climatic zones within a city based on the climate of local zones. These standards are globally uniform and do not change across regions.

Landsat 8 and 5 satellite images were used in the SAGA-GIS software environment to estimate land use changes for 17 urban classes, including various types of buildings with different densities and floors, industrial use, and natural and agricultural areas (Stewart and Oke, 2012; Stewart et al., 2014)(. For Landsat 8 satellite images, 9 bands (9–10, 1 to 7) with cloud cover less than 10% were utilized. For Landsat 5 images, bands of red, green, blue, and thermal were used. The inclusion of thermal bands allows for the differentiation of land uses based on temperature anomalies and microclimates.

Access to terrestrial data is required for this method due to the nature of the classes used. While some data can be manually obtained using Google Earth, other data, such as statistics for residential and industrial areas (including the number of floors in each area of Tehran), necessitate field surveys. The Tehran Municipality provides block statistics in the form of shapefiles. For more detailed information on this method and the definitions of different LCZ classes, please refer to Stewart et al. (2014). Three study periods (2000, 2010, and 2020) were considered to analyze LCZ for Tehran, and the transformation of different classes established during these periods is shown in Fig. 2. In the following the flowchart of the different stages of the research is presented in Fig. 3.

5. Results

5.1. Analysis of the frequency of occurrence of heat waves in Tehran

In this study, during the years 2000 to 2020, about 52 heat waves with durations of 3 to 18 days were identified. In total, heat waves with a duration of 3 days are the most abundant with 13 periods, then heat waves with a duration of 4 days were identified for 11 periods. For each of 10 to 14 and 18 days, only one study period was identified (Fig. 4a). In Fig. 4a, the number of occurrences of heat

Table 1
Suitable normalized difference vegetation index (NDVI) ranges were identified for the land cover classes (Akbar et al., 2019).

Class	NDVI value
Water	−0.28–0.015
Built-up	0.015–0.14
Barren land	0.14–0.18
Shrub and grassland	0.18–0.27
Sparse vegetation	0.27–0.36
Dense vegetation	0.36>

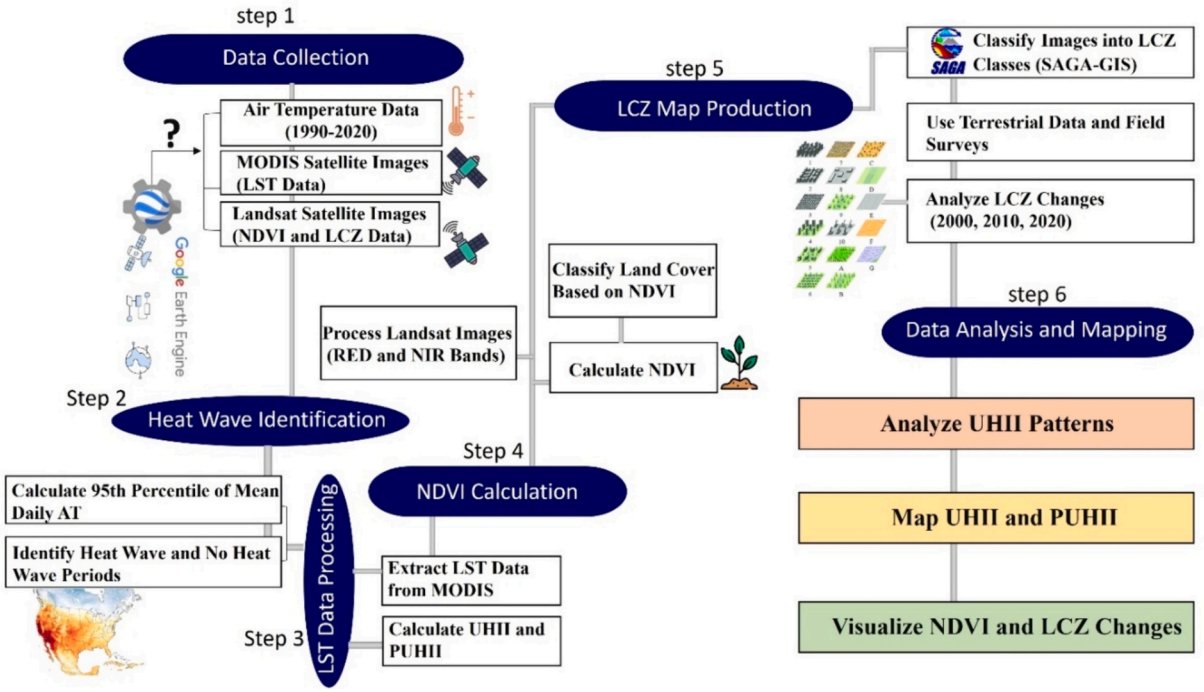

Fig. 3. Flowchart of various stages involved in research study.

waves with different daily durations is displayed. Fig. 4b also shows the frequency of occurrence of heat waves with different durations during the study years.

Based on this figure, it is clear that the years 2004, 2017 and 2020 are among the years for which the occurrence of heat waves has not been detected. However, 2011 with 8 waves, 2014 with 6 occurrences and 2006 with 5 occurrences of heat waves are in the first to third ranks. On the other hand, the longest heat wave was observed in 2003, with a duration of 18 days, then in 2018, a duration of 14 days, in 2009 and 2010, respectively, with a duration of 13 and 12 days. In general, based on Fig. 4b, it is clear that the daily continuity of heat waves in Tehran has increased since the second decade of studies.

In this study, only heat waves were selected for study when the cloudiness of the sky was less than 10%. This caused the number of selected heat waves to decrease. On the other hand, the study of all heat waves increases the output and complexity of the content, and more space should be allocated for the analysis of the findings, which led to only 25% of the heat waves (a quarter) being selected for this study. In Table 2, the mean daily AT for the period of occurrence of selected heat waves is presented along with the period without their heat waves. The mean daily AT for 13 heat wave events is 33.4 °C, which is 27.2 °C for the period before the heat wave. As can be seen, the mean daily AT during a heat wave is about 6.2 °C higher than the period without a heat wave. In the Fig. 5, selected heat waves are displayed.

5.2. Monitoring the spatial-temporal patterns of Tehran's UHI at the same time and before the heat wave event

It is necessary to explain that due to the limited space of the research and the reduction of the complexity of the content, averages are taken from the 13 studied cases, and the outputs will be interpreted based on the average maps.

At this stage, the pattern of LST changes before and simultaneously with the heat wave of Tehran city is presented. As the results show, the average LST according to 13 study events before the occurrence of the heat wave is 23.05 °C, and at the time of the occurrence of the heat wave, it is 26.39 °C. The results show that in all 13 studied periods, the LST at the same time as the heat wave occurs is higher than the LST before the heat wave occurs. So that this increase in LST varies from a minimum of 0.55 °C to a maximum of 8.61 °C, and its average value is 3.34 °C.

In Fig. 6, the LST spatial pattern is displayed for the period before the heat wave and at the same time as a heat wave. In total, according to the overall average of all studied cases, it can be seen that before the heat wave, the LST values fluctuated from a minimum of 16.33 °C to a maximum of 25.84 °C in Tehran. However, at the same time as the heat wave occurs, LST fluctuations are zoned from a minimum of 19.84 °C to a maximum of 28.92 °C throughout the city of Tehran. For both study times, it can be seen that the northern belt and cores (zone) in the southeast of Tehran experienced the minimum LST values and the maximum is related to the central areas that spread toward the east of Tehran (Fig. 6a, b).

Fig. 7a shows the comparison of the area (percentage) of different temperature classes (LST) throughout the city in times without and concurrent with the heat wave. From this figure, it can be seen that the skewness of the LST curve for the period at the same time as the heat wave occurred tended more to the right. In fact, this means that for the period of heat wave occurrence, an area of the city

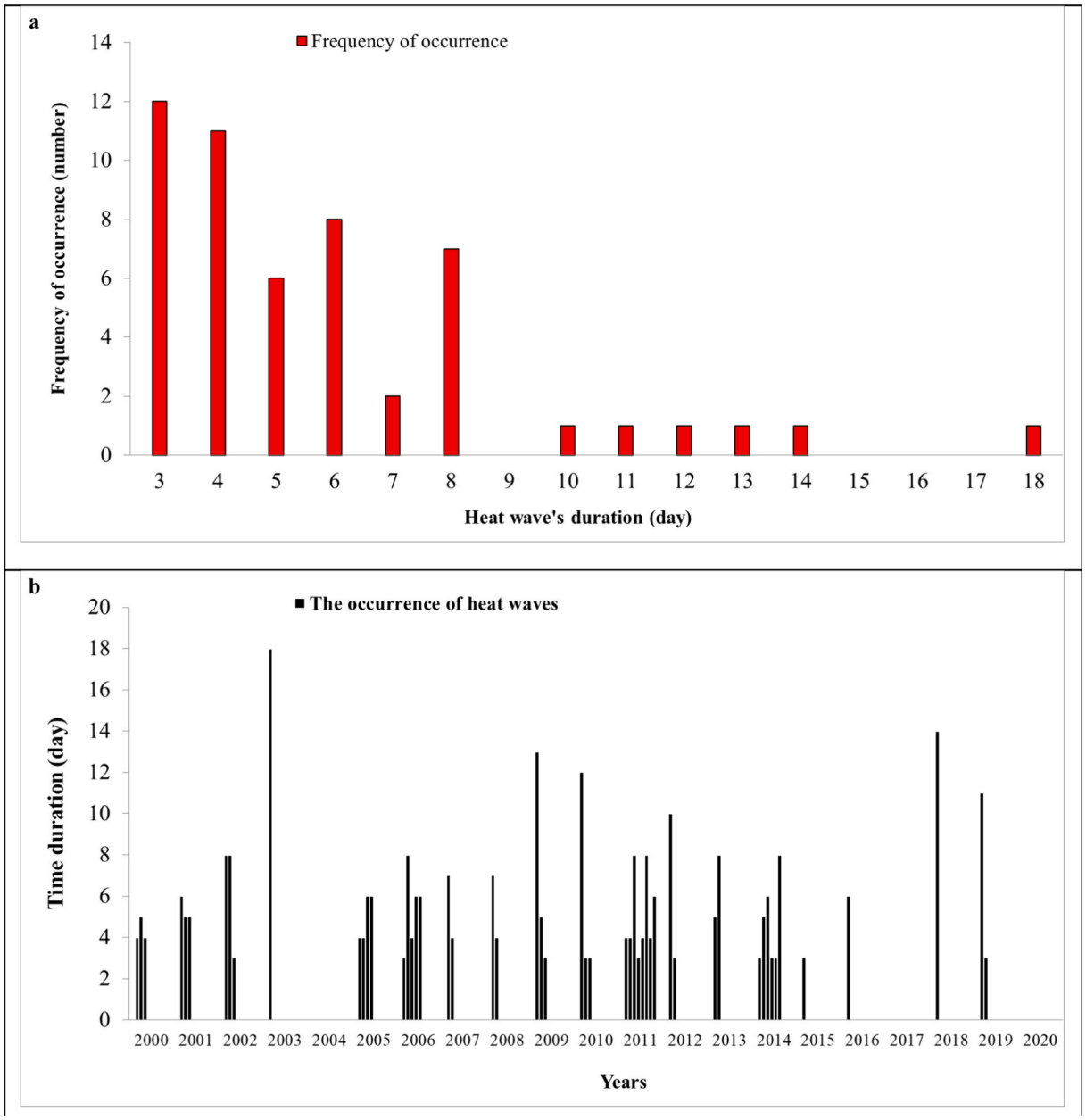

Fig. 4. (a) Frequency of heat waves with different periods. (b) Annual frequency of heat waves with different periods.

whose LST has more temperature thresholds has a larger width compared to the period without heat wave occurrence. As the results show, the frequency of LST classes of 16 to 22 °C and 22.1 to 29 °C, respectively, for the period without the occurrence of a regional heat wave, is equivalent to 24.73% and 75.27% of the area of Tehran, while the area of these classes for the period with the occurrence of the heat wave, it includes 0.40% and 99.60%. The difference of LST at the same time as the heat wave event compared to the period before the wave shows that there is an increase in LST from at least 2.44 °C to 4.42 °C in the over city.

According to Fig. 6c, it can be seen that the maximum rate of LST increase is for the northern strip of Tehran city, with a greater concentration for the northeast. On the other hand, the minimum LST increase is spread in the form of cores (zones) in the city, which are mainly concentrated in the west, south and southeast of Tehran.

Nevertheless, in the following, we can refer to the variability pattern of UHII for the period without a heat wave and simultaneously with the occurrence of a heat wave. It is necessary to remember that Eq. 2 was used for the zoning of the UHII map. So that for each pixel, a different value of UHII was extracted and based on them, a UHII map was prepared. The outputs in this regard show that the average UHII value for the period without a heat wave is 5.11 °C, while during the heat wave, its rate is 3.62 °C.

The results show that in all 13 studied periods, the UHI at the same time as the occurrence of a heat wave had a lower intensity

Table 2
The mean daily AT for the period without heat waves and simultaneously with selected heat waves. Continuity of heat wave (COHW); Air temperature during heat wave (ATDHW); Air temperature during no heat wave (ATDNHW); ΔTa = ATDHW - ATDNHW.

The case number	The date no heat wave (NHW)	The duration (day) of the heat wave (HW) event	COHW (days)	Mean ATDHW (°C)	Mean ATDNHW (°C)	ΔTa (°C)
1	2000-06-14	(2000-06-21 to 2000-06-24)	4	33.3	19.4	13.9
2	2001-08-17	(2001-08-20 to 2001-08-24)	5	33.4	28.4	5.0
3	2002-07-29	(2002-08-22 to 2002-08-24)	3	32.9	28.2	4.7
4	2005-06-28	(2005-07-04 to 2005-07-07)	4	33.5	27.5	6.0
5	2006-06-07	(2006-06-22 to 2006-06-29)	8	33.1	26.1	7.0
6	2006-07-02	(2006-07-07 to 2006-07-10)	4	35.1	27.3	7.8
7	2006-07-13	(2006-07-24 to 2006-07-29)	6	33.5	28.5	5.1
8	2007-06-05	(2007-06-13 to 2007-06-19)	7	32.9	24.5	8.4
9	2010-06-25	(2010-06-28 to 2010-07-12)	15	34.9	29.0	6.0
10	2011-07-29	(2011-07-31 to 2011-08-08)	9	33.6	29.6	4.0
11	2012-06-24	(2012-07-05 to 2012-07-14)	10	33.2	27.4	5.8
12	2015-08-10	(2015-08-17 to 2015-08-19)	3	32.3	27.9	4.4
13	2018-07-05	(2018-07-17 to 2018-07-27)	11	33.0	30.0	2.9

Table 3
LST and UHII values for the period without heat waves and simultaneously with selected heat waves.

The case number	Mean LST in duration of NHW (°C)	Mean LST in duration of HW (°C)	Mean UHII in duration of NHW (°C)	Mean UHII in duration of HW (°C)
1	19.08	25.10	4.33	3.89
2	23.56	25.97	4.25	3.86
3	24.03	24.58	11.36	3.49
4	20.34	26.39	3.77	3.60
5	25.18	27.38	3.77	3.60
6	24.67	26.84	4.55	4.12
7	17.56	26.16	5.61	3.75
8	24.37	28.09	3.96	3.29
9	21.30	24.39	3.46	3.33
10	25.66	27.09	3.81	3.46
11	23.31	26.15	3.56	3.49
12	24.23	26.71	10.09	3.58
13	26.40	28.21	3.87	3.55
Average	**23.05**	**26.39**	**5.11**	**3.62**

compared to the period without the occurrence of a heat wave, so from the examination of these 13 cases (Fig. 6f), it is clear that the minimum and maximum reduction of the UHII, respectively it includes −0.06 °C and −7.87 °C (Fig. 6d, e). In studies similar to our research results around the world, it has been determined that the UHII has decreased during the occurrence of heat waves (Scott et al., 2018; Chew et al., 2021; Miao et al., 2022).

However, contrasting results are reported as to whether UHI intensity (UHII) is exacerbated or reduced during heat waves. Based on this, we can refer to the result of a study for the city of Berlin during the years 2015 to 2018. So that, identifying the 10% hottest days or nights during May – September as hot weather episodes based on daytime conditions or inner-city nighttime conditions exacerbates nighttime UHII, while identifying them based on nighttime conditions at rural sites reduces it (Fenner et al., 2019).

At the same time, changes in UHII (decrease or increase) are associated with prevalent weather conditions such as radiation, cloud cover, wind speed, precipitation, and humidity, indicating that future changes in weather due to climate change will impact UHIIs and heat-stress hazards in cities, in addition to land cover changes (Fenner et al., 2019; Zheng et al., 2023; Lokoshchenko and Alekseeva, 2023; Liao et al., 2023).

Fig. 7b shows the comparison of the frequency of different UHII temperature classes throughout the city of Tehran in times without heat waves and simultaneously with heat waves. From this figure, it can be seen that for the period without heat waves, the skewness of the UHII curve tended to be more to the right. In fact, it can be observed that for the period without heat wave occurrence, the area where the UHI has a higher temperature intensity has covered a larger width of the city. So, the maximum frequency of UHII for the period without heat wave is 21.3% of the area of Tehran, corresponding to the temperature class of 8 °C. However, at the same time as the heat wave, this maximum frequency was experienced at 23.9% for the temperature class of 6 °C(Fig. 7b).

In Fig. 6d,e, the spatial pattern of UHII is displayed for periods without heat waves and simultaneously with heat waves. For both study times, it can be seen that the northern and small nuclear zones in the south of Tehran experienced the minimum UHII and the maximum intensity was assigned to the central areas of the city. It is worth considering that on average, 0.40% of the area of Tehran city and 1.9% of the area of the city during the heat wave have experienced a decrease in UHII compared to the suburbs (Fig. 6f).

It can be seen from the map of the difference in UHII for the simultaneous heat wave compared to the period without heat wave that the UHII did not experience any positive values throughout the area of Tehran (Fig. 6f). In other words, all areas of Tehran city have had less UHII during the heat wave period. The minimum and maximum rate of reduction of UHII throughout the city has fluctuated

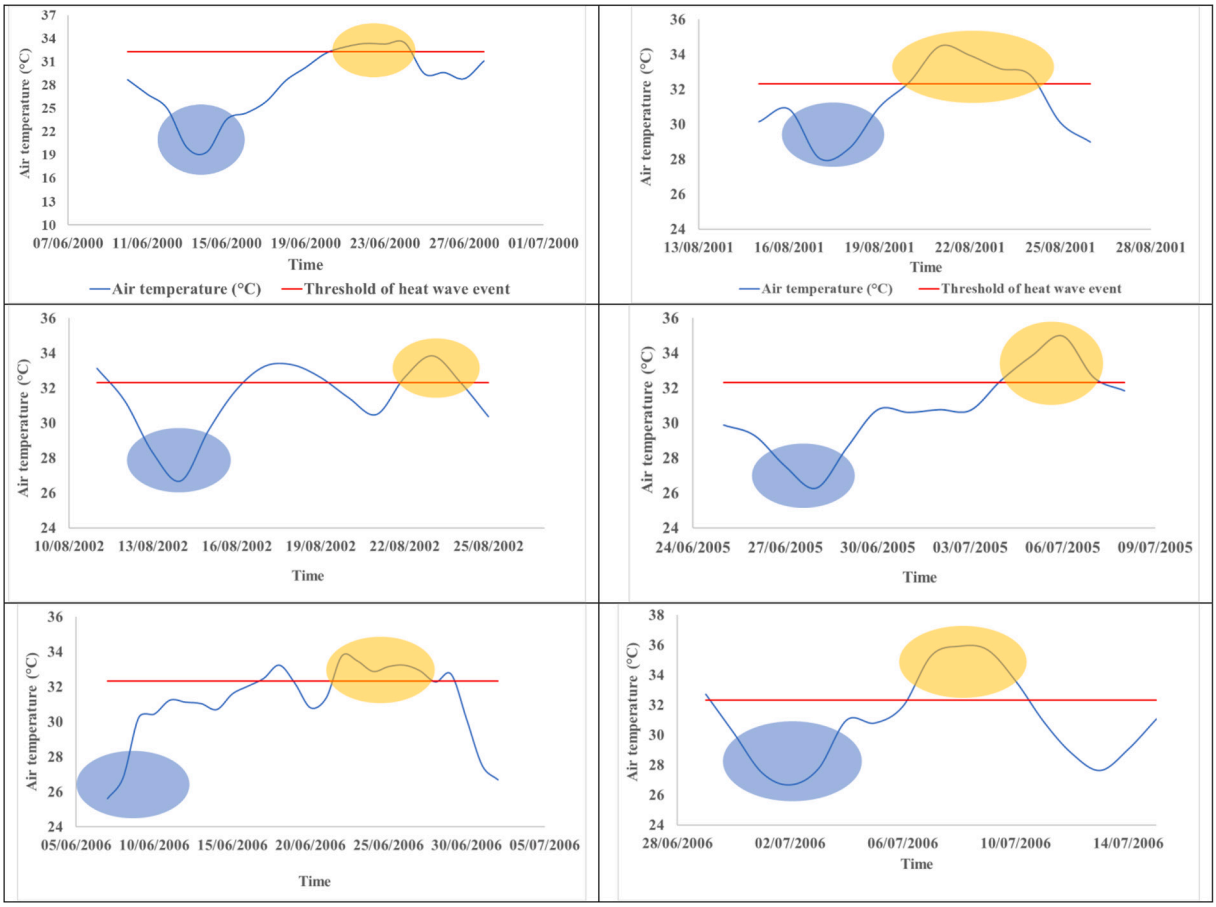

Fig. 5. Change of air temperature pattern in the period before and simultaneously with the occurrence of selected heat waves.

from −0.6 °C to −2.6 °C (Fig. 6f). At the same time, according to Fig. 6f, it is clear that the lowest rate of decrease in UHII is for the northern strip of Tehran, with more concentration for the northeastern areas. On the other hand, the south and southeast of Tehran have experienced the greatest decrease in UHII during the heat wave period in comparison to the period without heat wave occurrence. It is worth noting that Fig. 7c displays a comparison of the differences in the UHII between periods of heat wave occurrence and periods without heat wave occurrence for 13 case studies.

5.3. *Evaluating the role of local climate zones on the difference in UHII pattern*

Our investigations show that the UHII threshold of all the study cases for LCZs without man-made structures (Dense trees, Scattered trees, Bush, scrub, Low plants, Bare soil or sand, Water) have lower values than it shows to other land users (Fig. 8). These conditions are observed for both periods without wave and heat wave. In general, for the heat waveless period, Case 12, which corresponds to the date 2015-08-10, shows the maximum UHII for all LCZs. For this date, the maximum value of UHII with 11.12 °C is assigned to Compact midrise. The minimum UHII for this date with a value of 5.49 °C is assigned to Bush, scrub. For the same period as the wave event, case 6, which is equivalent to 2006-07-07 to 2006-07-10, has experienced the maximum UHII in all land uses that are not man-made (Fig. 8).

According to the overall average UHII of all land uses, it can be seen that in the period without heat waves, the minimum and maximum UHII values are 0.76 °C and 5.57 °C, respectively, corresponding to Bush, scrub and Compact midrise. For the same period as the heat wave, the minimum UHII of 0.52 °C was assigned to Bush, scrub, and the maximum value of 4.70 °C belonged to Compact midrise. For both study periods, after the use of Compact midrise, the maximum UHII is seen for Heavy industry, sparsely built and Large low-rise. On the other hand, in both study periods, after using Bush scrub, the minimum UHII belongs to Bare soil or sand. However, there are some differences in the ranking of UHII between different uses two times before and simultaneously with the heat wave.

As an example, for the period without a heat wave, the Dense Trees user is in third place (from low to high), while this user is in fourth rank at the same time as the heat wave occurs. Alternatively, for the period before (without) the heat wave, the Open midrise

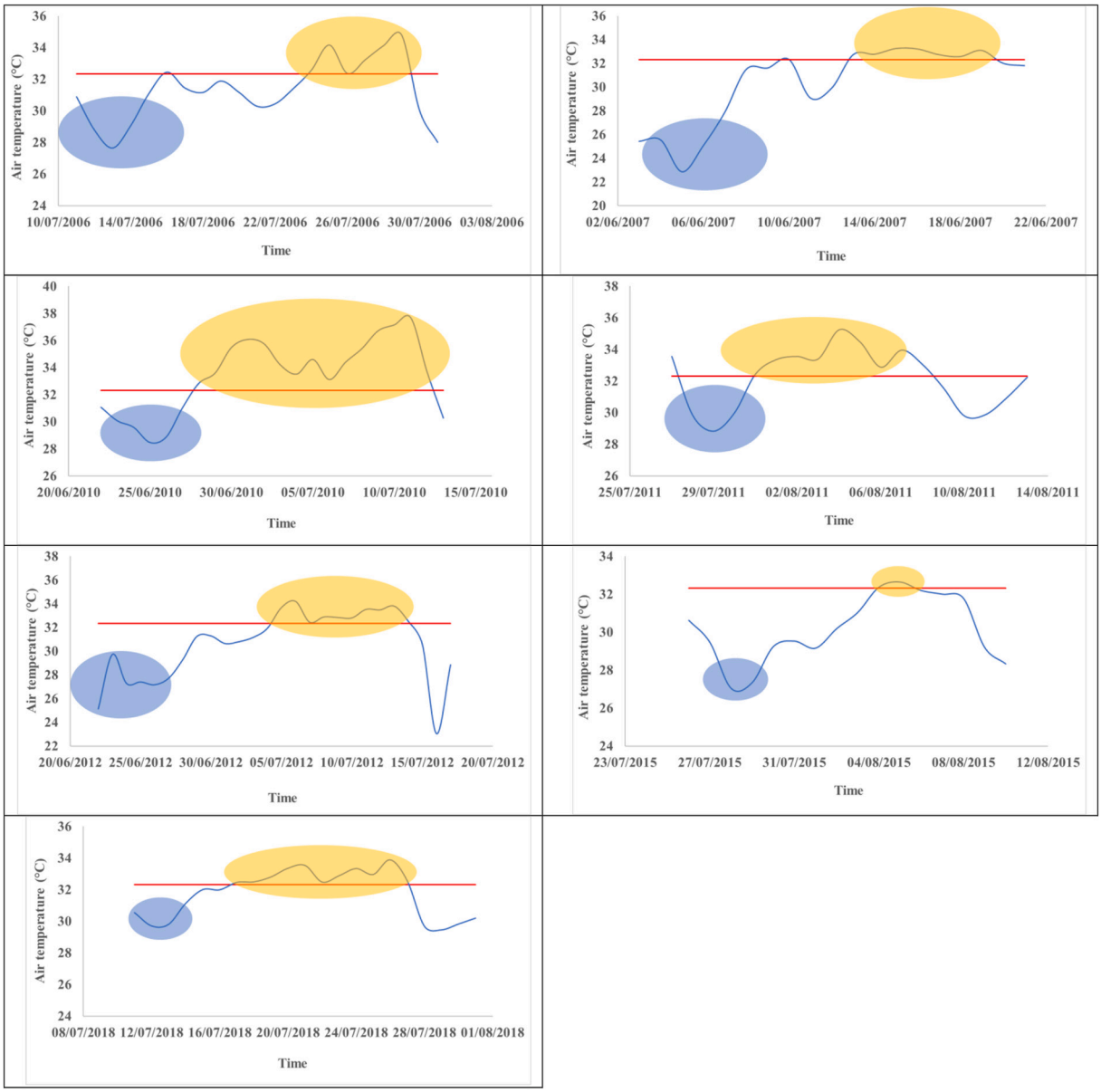

Fig. 5. (*continued*).

and Open low-rise uses are ranked 7 and 8, respectively. Still, at the same time as the Open low-rise heat wave occurred, the seventh and eighth rank was assigned to Open midrise. In total, in both study periods, a slight difference can be seen regarding the ranking of different land uses in terms of the UHII. The findings of this part of the research show that in all land uses, the UHII during a heat wave is lower than during the period without a heat wave (Fig. 9).

Nevertheless, based on the obtained results, it is clear that the highest rate of increase in the UHII for the period without a heat wave compared to the period of the occurrence of a heat wave is 1.12 °C, 1.05 °C and 1.03 °C respectively, for Water, Open midrise and Low plants and for Sparsely built uses, Compact midrise and Large low-rise with values of 0.24 °C, 0.33 °C and 0.43 °C have experienced the lowest increasing rate of UHII (Fig. 9). In many other researches, it has been determined that the difference in the land use of cities affects the severity of the UHI.

In all these studies (Mohan et al., 2013; Stache et al., 2022; Rahaman et al., 2022; Rendana et al., 2023), it is clear that vegetation and water uses have experienced the least UHII in comparison with other man-made uses. On the other hand, the studies that are focused on the city of Tehran clearly show that there is an inverse relationship between the NDVI index and the UHII (Bokaie et al., 2016; Tayyebi et al., 2018; Arghavani et al., 2021).

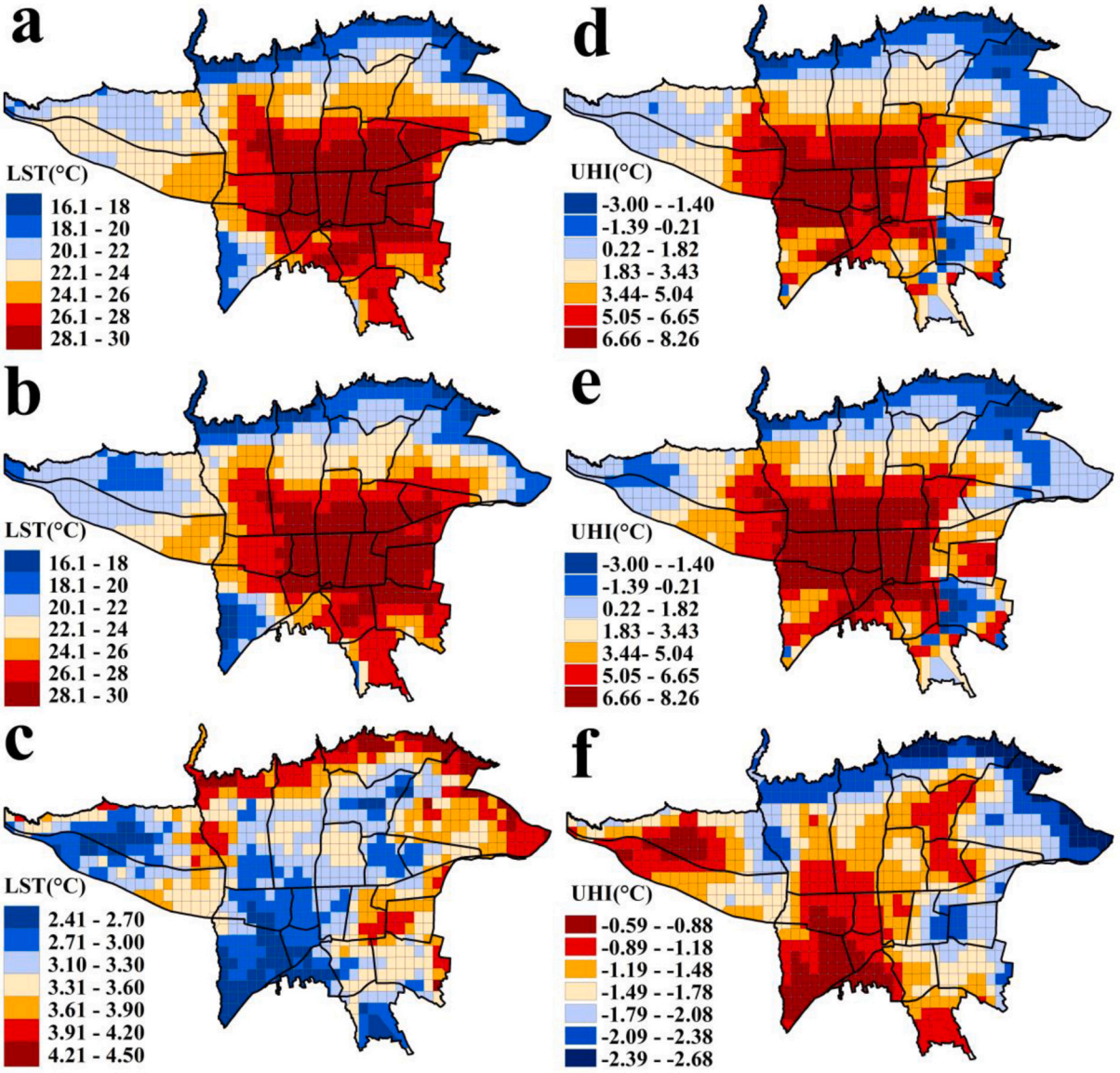

Fig. 6. The map of average LST spatial changes for (a) period without a heat wave, (b) concurrent with a heat wave event and (c) the LST difference of the period concurrent with a heat wave event from the period without a heat wave. Spatial change map of UHII for (d) period without a heat wave, (e) at the same time as the occurrence of a heat wave and (f) the difference of the UHII of the heat wave period from the period without a heat wave.

5.4. Evaluation of the role of vegetation on the UHII pattern

In this part of the study, NDVI monitoring was done for all study periods. The time interval between the heat wave occurrence period and the non-heat wave period is very short. Therefore, no difference in NDVI values can be observed. In this work, the average NDVI was considered for the period from the beginning of the non-heat wave period to the end of the heat wave period. So, this process was done separately for all 13 case studies.

In all the studied cases, the areas with vegetation cover have experienced the maximum NDVI value and the areas with man-made use have the minimum NDVI. Since the spatial pattern of these 13 cases is similar, and due to the limited length of the article, only the average of these 13 study periods was used to prepare the NDVI map (Fig. 10). In this figure, the maximum NDVI values belong to the area of the north, west and southeast of Tehran. On the other hand, the central areas of the city, which are mostly dedicated to man-made uses, have experienced the minimum NDVI. In this study, the changes in the UHII behavior pattern for the period non-heat wave (and simultaneously with the heat wave) were compared with the change in the NDVI behavior.

In this part of the study, it was found that there is an inverse relationship between NDVI and UHII throughout the city of Tehran,

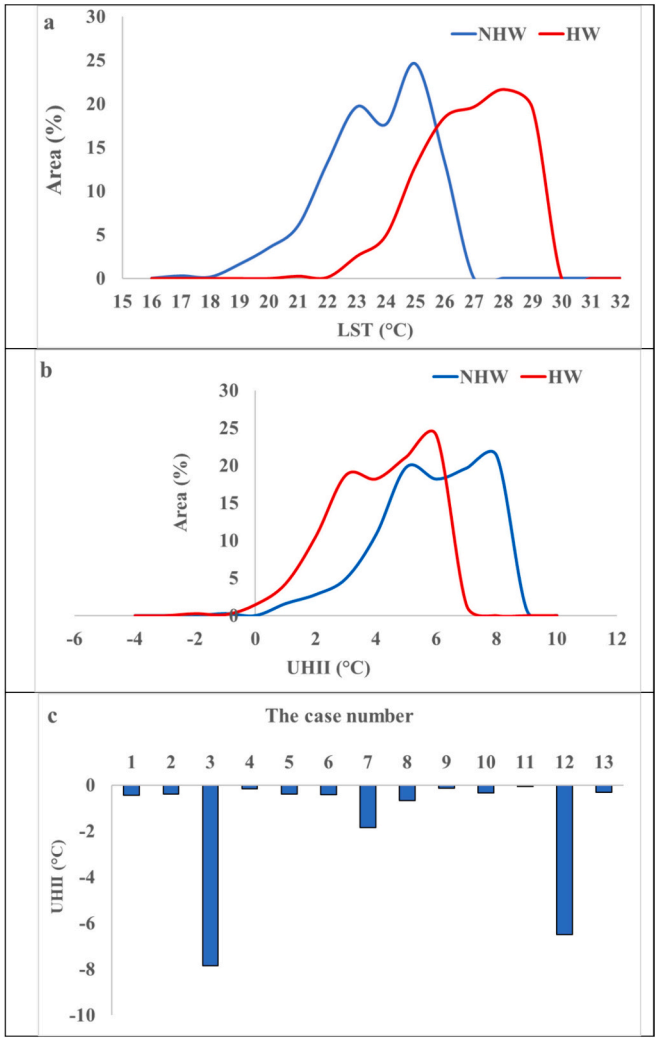

Fig. 7. Comparison of the area (percentage) of temperature classes for (a) LST and (b) UHII during the without heat wave period and at the same time as the heat wave. (c) Comparing the difference in UHII between the period of heat wave occurrence from the period without the occurrence of heat wave for 13 case studies (in Table 3), the time of occurrence of each heat wave event is specified according to the case number).

and this behavior is observed for both periods of non-heat waves and at the same time with heat waves with a very small difference. According to Fig. 11, it can be clearly seen that the changes in UHII behavior are affected by the changes in NDVI, so with the increase in NDVI, the values of UHII decreased. The value of $R^2 = 0.17$ and $R^2 = 0.18$, respectively, for the period non-heat wave and simultaneously with the heat wave, together with p-value $= 0.0000$, confirms the significance of these changes at the level of 0.95%. In summary, it can be acknowledged that in confirming the results of LCZ, the green cover of the urban space is effective in adjusting the heat budget and reducing the intensity of the heat island.

5.5. *Evaluation of the role of heat waves on LST and UHII changes*

As part of the research, LST and UHII changes during the nighttime were compared with the air temperature during the nighttime. Results indicate that in the time before the heat wave, the LST was, on average, 1.51 °C higher than the air temperature at nighttime. But during the heat wave period, the LST is on average, −0.26 °C lower than the nighttime air temperature (Fig. 12a). The result shows that during the heat wave occurrence, the difference between LST and AT decreases compared to the period before the heat wave occurrence due to the stability of the air. In normal climatic conditions without heat waves, the average LST during the nighttime was higher than the AT during the nighttime. Urban construction materials such as asphalt, concrete and steel are the main reason for that due to their ability to absorb and store heat (Li et al., 2024). These materials absorb heat during the day and slowly release it during the night. Therefore, the surface temperature of the earth can remain high at night, while the air temperature can decrease. However during the heat wave occurrence, the stability of the atmospheric conditions prevents the sharp decrease of the night air temperature. It causes the air temperature to be higher than the LST at some times.

	LCZs	Case 1	Case 2	Case 3	Case 4	Case 5	Case 6	Case 7	Case 8	Case 9	Case 10	Case 11	Case 12	Case 13
No heat wave	Compact midrise	5.88	5.47	4.60	5.22	4.87	4.73	5.12	6.53	5.15	5.00	3.91	11.12	4.83
	Open midrise	3.67	3.43	2.60	3.44	2.88	3.86	2.99	4.80	3.01	2.81	2.09	9.19	3.01
	Open low-rise	3.25	3.36	2.77	3.45	2.84	3.58	2.96	4.91	2.97	3.07	3.00	9.18	3.26
	Large low-rise	2.96	3.75	3.67	2.75	3.26	5.01	3.10	5.72	2.98	3.40	4.26	10.03	3.60
	Sparsely built	3.79	3.82	3.47	3.92	4.26	3.72	3.58	5.45	4.13	3.31	3.14	10.34	3.47
	Heavy industry	4.08	4.36	3.95	3.99	4.16	4.60	3.88	5.69	4.24	3.94	4.42	10.42	4.00
	Dense trees	3.52	2.47	0.65	2.99	-0.15	3.20	1.97	4.20	2.01	2.02	1.44	7.91	2.12
	Scattered trees	2.75	2.89	2.11	3.19	2.26	4.56	2.24	4.91	2.86	2.47	3.01	8.72	2.96
	Bush, scrub	1.52	0.16	-0.98	1.47	-1.15	0.93	0.12	2.13	-0.11	-0.11	0.25	5.49	0.12
	Low plants	1.46	2.00	2.10	2.73	2.51	3.05	1.81	4.62	2.94	1.93	3.75	9.59	1.94
	Bare soil or sand	0.04	0.14	-0.10	1.60	-0.37	2.24	0.18	1.81	-0.23	0.16	0.38	6.60	0.28
	Water	1.33	2.09	2.26	3.24	2.52	4.36	1.46	5.17	3.25	1.88	3.73	8.95	3.73
Heat wave	Compact midrise	5.33	4.84	4.92	4.65	5.47	4.36	4.69	4.98	4.38	4.57	3.87	4.55	4.47
	Open midrise	3.35	3.24	3.09	2.70	3.33	3.31	2.80	2.93	2.66	2.77	2.89	2.85	2.65
	Open low-rise	2.96	3.22	2.94	2.95	3.37	3.27	2.85	2.90	2.60	2.71	2.85	3.00	2.93
	Large low-rise	2.42	3.77	2.56	3.19	3.57	4.52	2.69	3.12	2.60	2.74	3.29	3.04	3.36
	Sparsely built	3.48	3.68	3.31	3.79	3.80	3.36	3.15	3.43	2.94	3.18	3.08	3.18	3.17
	Heavy industry	3.54	3.97	3.59	4.20	4.24	4.17	3.68	3.83	3.20	3.46	3.94	3.62	3.76
	Dense trees	2.75	2.99	2.56	2.31	1.50	3.19	2.11	2.07	2.05	2.19	1.98	2.20	2.10
	Scattered trees	2.50	3.01	2.44	2.66	2.55	3.95	2.45	2.27	2.09	2.17	3.05	2.65	2.62
	Bush, scrub	0.60	1.46	0.86	-0.14	0.39	1.65	0.27	0.17	0.36	0.28	0.59	0.21	0.02
	Low plants	1.26	1.95	1.45	2.83	1.92	3.15	1.55	1.65	1.42	1.57	3.92	1.43	1.82
	Bare soil or sand	0.47	1.44	0.27	0.07	0.38	2.06	0.15	0.02	0.31	0.15	1.29	0.46	0.10
	Water	1.72	2.29	1.43	2.73	1.94	3.80	2.17	1.86	1.56	1.59	3.30	2.99	3.19

Fig. 8. UHII according to different LCZs of no-wave period and simultaneously with heat wave occurrence for 13 studied cases.

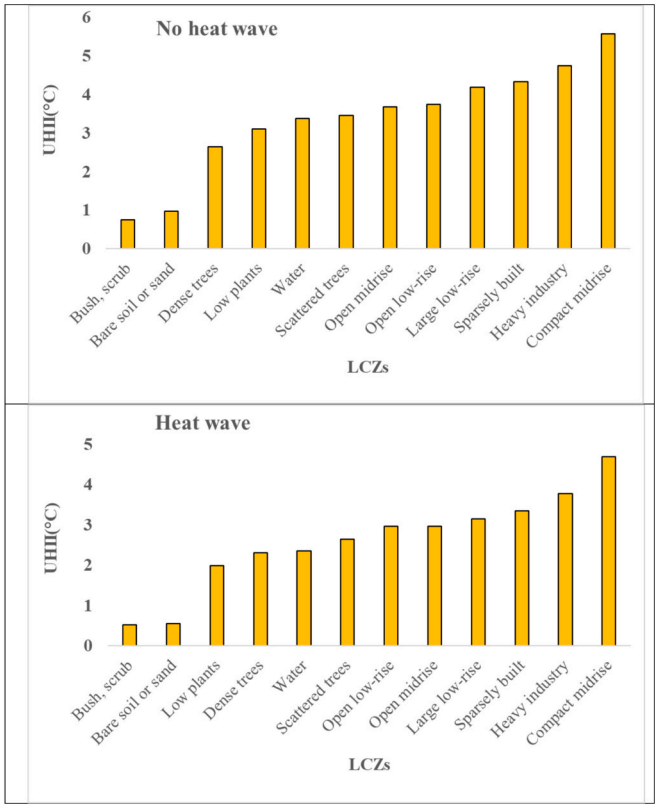

Fig. 9. The average UHII according to different LCZs for the period without a heat wave and simultaneously with the occurrence of a heat wave.

Next, the correlation between nighttime AT and UHII was taken. According to Fig. 12b,c, it can be seen that the value of $r = 0.60$ (significance at the 95% level) for the time of the heat wave occurrence and $r = 0.26$ for the period before the heat wave. Fig. 12b and c show that the UHII changes have a direct and significant effect from the heat wave event. However, for the times without the heat wave event, although there is a direct relationship between AT and UHII, these changes do not have a significant level, and it seems local factors have a more important role in controlling the UHII.

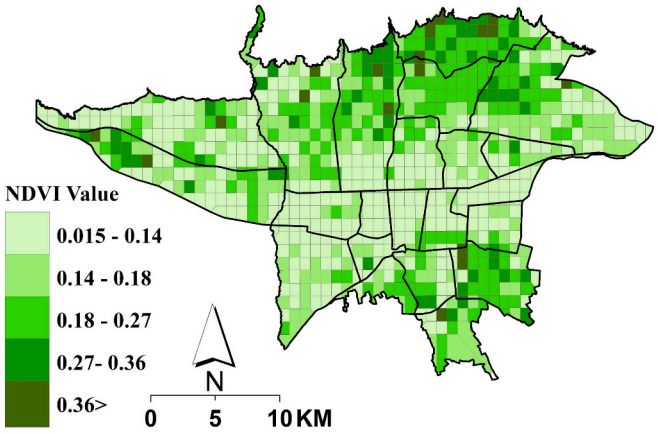

Fig. 10. Average spatial changes of NDVI over the city of Tehran according to selected study periods.

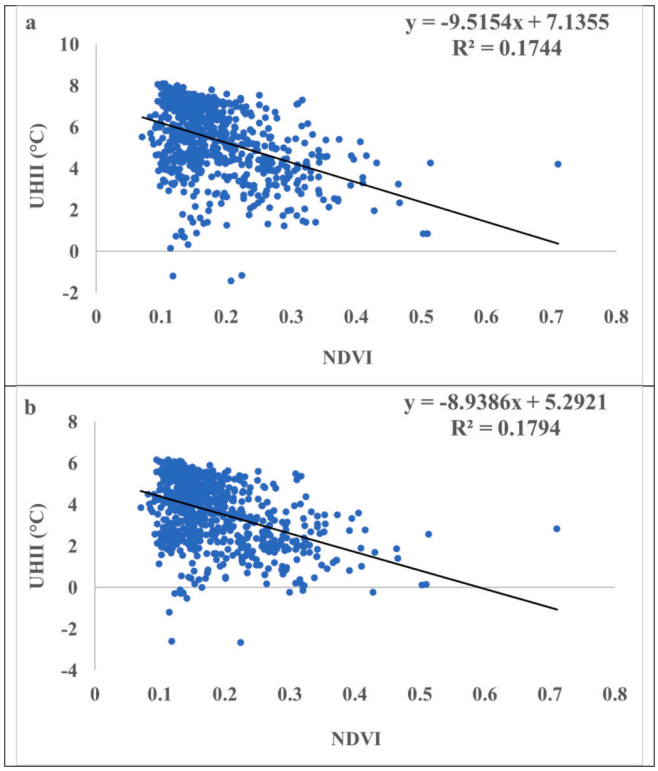

Fig. 11. Behavioral comparison of the average UHII changes for (a) the period non-heat wave and (b) at the same time as the heat wave event with the average NDVI changes over the city of Tehran.

6. Discussion

This study was conducted in order to identify the effect of heat waves on the intensity of the urban heat island. The results of this research showed that the occurrence of a heat wave causes an increase in LST. The LST experienced a significant increase during the heat wave occurrence compared to the period without heat wave. This increase in LST during a heat wave can have different consequences, especially in terms of increasing energy demand in the cooling sector, increasing water use, or increasing medical emergencies. Undoubtedly, one of the solutions to adapt and reduce the negative effects of this climate disaster is the design and localization of heat wave warning systems (Kanti et al., 2022; Kiarsi et al., 2023), which requires city managers to integrate urban adaptability and resilience plan, invest and implement actions against this risk.

In the cities located in semi-arid continental climates, including Tehran, the consequences of global warming are translated into the

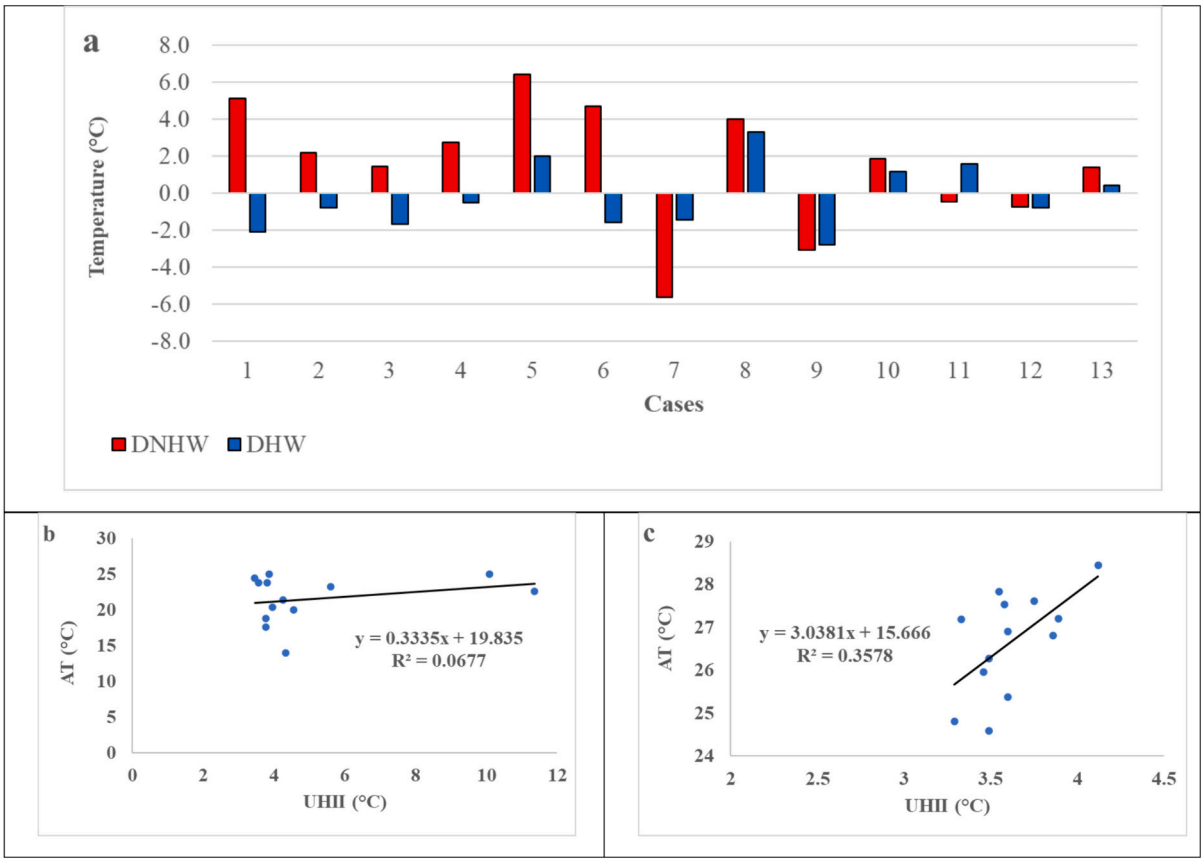

Fig. 12. Comparison of temperature difference between LST during heat wave event (DHW) and non-heat wave event (DNHW). Behavioral comparison between UHII and AT at the time (b) DNHW and (c) DHW during the nighttime for 13 studied cases.

increase in the occurrence of heat waves. Its direct effects are the increase in death rates or the referral of patients to emergency medical centers, especially in large populated cities (Wang et al., 2023; Wedler et al., 2023). All these consequences can cause additional costs for governments. Additional costs would better be invested in the adaptation of cities to climate change so that, in the long run, the vulnerability of the urban society will be reduced. Furthermore, all citizens can benefit from its benefits.

Despite the conclusion that the occurrence of a heat wave can lead to an increase in LST, it may be assumed that the UHII can also increase with the occurrence of this weather disaster. The findings of this research showed that during the occurrence of a heat wave, the UHII decreased compared to the period without a heat wave. In fact, at the time of heat wave occurrence, a warm atmospheric system covers a wide area in the dimensions of synoptic studies. During this period, the temperature difference between the suburbs and the urban environment has decreased, and the result is a decrease in thermal UHII. In other words, extra-local (synoptic) factors can be effective in reducing the contribution of local components (such as land use) in controlling the UHII. As Van Tol and Ellis (2023) showed, for American cities, increasing the persistence of warm weather types in some places is unlikely to have a direct effect on the average UHI intensity.

At the same time, the percentage of influence of extra-local (synoptic) factors in reducing the share of local factors depends on various parameters such as the intensity, duration and duration of the weather disaster (heat wave) and even as it has been determined, the climate type of the region (Chew et al., 2021) can be influential in the contradiction of the results. Of course, this is not a general rule, and it may be similar to the findings of some studies (Anjos et al., 2020; Półrolniczak et al., 2017) that extra-local (synoptic) factors increase the UHII because it seems that atmospheric circulation is significantly responsible for the formation and evolution of meteorological elements that can impose or eliminate the phenomena (Mihalakakou et al., 2002).

So, for this purpose, it is suggested to pay attention to the effect of heat waves on the change of the UHII pattern in the next studies with a synoptic approach. The findings of this research showed that UHII is different according to the type of different uses. The study findings indicate that man-made uses experienced maximum UHII in both periods without and simultaneously with the heat wave. It is noteworthy that at night, the minimum UHII belongs to the areas with the least vegetation and bare soil or sand. In fact, these areas lose heat energy faster than other uses and are cooler than other areas due to the fact that they are not assigned to man-made uses and, on the other hand, due to the small amount of vegetation. Although urban sprawl can increase the temperature of city areas, it seems that with the change in the use of suburban areas, the temperature difference between these two areas will decrease (Leichenko and Solecki, 2013; Mansouri Daneshvar et al., 2019).

This can have different effects on changing the microclimatic pattern of different areas of the city. For example, the temperature difference can affect the pressure difference and, finally, the flow of local winds. However, with the reduction of the temperature difference between the urban area and the countryside, it is expected that the pattern of local winds will change, and their intensity will decrease to some extent. Since the wind blowing in urban areas can lead to a decrease in the heat budget and, on the other hand, a decrease in pollutants, then the decrease in the intensity and frequency of local winds can result in an increase in the city's heat budget and an increase in the concentration of urban pollutants and ultimately negative environmental effects.

Future work should focus on the identification of hot spots using high-resolution mapping techniques based on field measurements and surveys. Perhaps one of the solutions to reduce the city's heating budget is to focus and invest in urban green space. As the results of this research showed, it can be seen that areas with denser vegetation have experienced less UHII compared to man-made environments.

Focusing on the expansion of urban green space is still introduced as one of the valuable solutions to adapt to climate change and its consequences, such as heat waves, as other studies have also pointed out its importance in reducing the urban heating budget. Semenzato et al. (2023); Zhou et al. (2023). Since the results extracted in this article are related to the nighttime, there is a possibility that different results can be extracted for the daytime hours. Future research should focus on studying the results of the influence of heat waves on the UHII during daytime hours and compare their findings with nighttime hours.

7. Conclusion

UHI has been one of the concerns around the world for more than a century. With the expansion of cities, especially in semi-arid continental climates, monitoring and evaluation of UHI and, on the other hand, UHII changes have become valuable tools for planning in urban environments in order to monitor and manage urban growth. This paper explains the UHII and temporal and spatial variations in response to LST during a heat wave in the metropolis of Tehran in Iran. 13 heat waves were selected and evaluated during the years 2000 to 2020.

The are three major findings identified in this article. First, the average LST was 3.34 °C higher during heat waves. Second, the research shows that despite the increase in LST during the heat wave occurrence, UHII experienced lower values compared to the time without the wave. Thirdly, findings indicate that during a heat wave, the temperature difference between AT and LST witness a greater decrease compared to the period non-heat wave, which can be due to the stability of the air during a heat wave. On the other hand, during a heat wave, there is a significant and direct relationship between AT and UHII, which did not have a significant level for the period of the non-heat wave. In other words, it can be concluded that the extra-local factor (atmospheric anomaly) has a significant effect on UHII during the heat wave event. In contrast, for the non-heat wave, the influence of local factors has a more effective role in controlling UHII.

The study found that high urban intensity in the city center of Tehran is associated with minimum NDVI values. The findings prove that the expected positive role of urban green vegetation and its influence in reducing heat stress in Tehran was insignificant due to the low NDVI values. A more diverse land use and the presence of open spaces with high vegetation density would have influenced the UHII.

Therefore, the introduction of green spaces in urban dense agglomerations should be part of any future climate change mitigation measure and action plan. Also, field surveys and local weather data should be further collected to better characterize the urban thermal layer in the capital of Iran and accurately define the hot spot using high-resolution spatial and temporal variability maps.

Funding

"This research received no external funding".

CRediT authorship contribution statement

Gholamreza Roshan: Writing – original draft, Validation, Supervision, Methodology, Investigation, Formal analysis, Conceptualization. **Saleh Arekhi:** Software, Methodology. **Zainab Bayganeh:** Resources, Data curation. **Shady Attia:** Writing – review & editing, Validation, Conceptualization.

Declaration of competing interest

The authors declare that they have no conflict of interest.

Data availability

Data will be made available on request.

Acknowledgments

We wish to thank Prof. Ghanghermeh from the Golestan University (Iran) and Reza Sarli from the University of Agriculture in Krakow (Poland) for their comments and intellectual guidance, which helped improve an earlier version of the paper.

References

Akbar, T.A., Hassan, Q.K., Ishaq, S., Batool, M., Butt, H.J., Jabbar, H., 2019. Investigative spatial distribution and modelling of existing and future urban land changes and its impact on urbanization and economy. Remote Sens. (Basel) 11, 105.

Alghamdi, A.S., Harrington, J., 2016. Synoptic climatology and sea surface temperatures teleconnections for warm season heat waves in Saudi Arabia. Atmos. Res. 216, 130–140.

Almusaed, A., 2011. The urban heat Island phenomenon upon urban components. Biophil. Bioclim. Arch. 21, 139–150.

Anderson, G.B., Bell, M.L., 2011. Heat waves in the United States: mortality risk during heat waves and effect modification by heat wave characteristics in 43 US communities. Environ. Health Perspect. 119, 210–218.

Anjos, A., Targino, A.C., Krecl, P., Oukawa, G.Y., Braga, R.F., 2020. Analysis of the urban heat island under different synoptic patterns using local climate zones. Build. Environ. 185, 107268.

Arghavani, S., Malakooti, H., Bidokhti, A.A., 2021. Evaluation the effects of urban green space scenarios on near-surface turbulence and dispersion related parameters: a numerical case study in Tehran metropolis. Urban For. Urban Green. 59, 127012.

Barati, G., Moradi, M., Saiidinya, M., 2021. Synoptic analysis of hottest cities in Iran. Res. Earth Sci. 12 (2), 64–73.

Bokaie, M., Zarkesh, M.K., Arasteh, P.D., Hosseini, A., 2016. Assessment of urban Heat Island based on the relationship between land surface temperature and land use/land cover in Tehran. Sustain. Cities Soc. 23, 94–104.

Cai, Z., Sorte, F.A.L., Chen, Y., Wu, J., 2023. The surface urban heat island effect decreases bird diversity in Chinese cities. Sci. Total Environ. 902, 166200.

Caldeira, D., Dores, H., Franco, F., Baptista, S.B., Cabral, S., Cachulo, M.D.C., Peixeiro, A., Rodrigues, R., Santos, M., Timóteo, A.T., Campos, L., Vasconcelos, J., Nogueira, P.J., Gonçalves, L., 2023. Global Warming and Heat Wave Risks for Cardiovascular Diseases: A Position Paper from the Portuguese Society of Cardiology. Revista Portuguesa de Cardiologia. https://doi.org/10.1016/j.repc.2023.02.002 in press.

Chen, H., Deng, Q., Zhou, Z., Ren, Z., Shan, X., 2022. Influence of land cover change on spatio-temporal distribution of urban heat island — A case in Wuhan main urban area. Sustain. Cities Soc. 79, 103715.

Cheval, S., Amihăesei, V.A., Chitu, Z., Dumitrescu, A., Falcescu, V., Irașoc, A., Magdalena Micu, D., Mihulet, E., Ontel, I., Paraschiv, M.G., Tudose, N.C., 2024. A systematic review of urban heat island and heat waves research (1991–2022). Clim. Risk Manag. 44, 100603.

Chew, L.W., Liu, X., Li, X.X., Norford, L.K., 2021. Interaction between heat wave and urban heat island: a case study in a tropical coastal city, Singapore. Atmos. Res. 247, 105134.

Cuerdo-Vilches, T., Díaz, J., López-Bueno, J.A., Luna, M.Y., Navas, M.A., Mirón, I.J., Linares, C., 2023. Impact of urban heat islands on morbidity and mortality in heat waves: observational time series analysis of Spain's five cities. Sci. Total Environ. 890, 164412.

Cui, F., Hamdi, R., Kuang, W., Yang, T., He, H., Termonia, P., De Maeyer, P., 2023. Interactions between the summer urban heat islands and heat waves in Beijing during 2000–2018. Atmos. Res. 291, 106813.

Dadashpoor, H., Alidadi, M., 2017. Towards decentralization: Spatial changes of employment and population in Tehran metropolitan region, Iran. Appl. Geogr. 85, 51–61.

Daniel, M., Lemonsu, A., Viguie, V., 2018. Role of watering practices in large-scale urban planning strategies to face the heat-wave risk in future climate. Urban Clim. 23, 287–308.

Daramola, M.T., Balogun, I.A., 2019. Local climate zone classification of surface energy flux distribution within an urban area of a hot-humid tropical city. Urban Clim. 29, 100504.

Darand, M., Halabian, A., 2013. Classification synoptic circulation patterns impacting on air pollution in Tehran. J. Appl. Sci. Res. 3 (5), 40–146.

Dezső, Z., Pongrácz, R., Bartholy, J., 2024. Surface urban heat island in Budapest during heat waves and droughts - comparing the summers of 2003, 2007 and 2022. Urban Clim. 55, 101899.

Fenner, D., Holtmann, A., Meier, F., Langer, L., Scherer, D., 2019. Contrasting changes of urban heat island intensity during hot weather episodes. Environ. Res. Lett. 14, 124013.

Firozjaei, M.K., Fathololoumi, S., Kiavarz, M., Arsanjani, J.J., Alavipanah, S.K., 2020. Modelling surface heat island intensity according to differences of biophysical characteristics: a case study of Amol city, Iran. Ecol. Indic. 109, 105816.

Foissard, X., Dubreuil, V., Quénol, H., 2019. Defining scales of the land use effect to map the urban heat island in a mid-size European city: Rennes (France). Urban Clim. 29, 100490.

Fonseca-Rodríguez, O., Adams, R.E., Sheridan, S.C., Schumann, B., 2023. Projection of extreme heat- and cold-related mortality in Sweden based on the spatial synoptic classification. Environ. Res. 239 (Part 2), 117359.

Ghanghermeh, A., Roshan, G., Orosa, J.A., Calvo-Rolle, J.L., Costa, Á.M., 2013. New climatic indicators for improving urban sprawl: a case study of Tehran City. Entropy 15, 999–1013.

Ghanghermeh, A., Roshan, G., Orosa, J.A., Costa, Á.M., 2019. Analysis and comparison of spatial–temporal entropy variability of Tehran City microclimate based on climate change scenarios. Entropy 21, 13.

Ghobadi, A., Khosravi, M., Tavousi, T., 2018. Surveying of heat waves impact on the urban Heat Islands: Case study, the Karaj City in Iran. Urban Clim. 24, 600–615.

Gogoi, P.P., Vinoj, V., Swain, D., Roberts, G., Dash, J., Tripathy, S., 2019. Land use and land cover change effect on surface temperature over Eastern India. Sci. Rep. 9 (1), 8859.

Good, E.J., Ghent, D.J., Bulgin, C.E., Remedios, J.J., 2017. A spatiotemporal analysis of the relationship between near-surface air temperature and satellite land surface temperatures using 17 years of data from the ATSR series. J. Geophys. Res. Atmos. 122 (17), 9185–9210.

He, S., Zhang, Y., Gu, Z., Su, J., 2019. Local climate zone classification with different source data in Xi'an, China. Indoor Built. Environ. 28 (9), 1190–1199.

Huynen, M.-M., Martens, P., Schram, D., Weijenberg, M.P., Kunst, A.E., 2001. The impact of heat waves and cold spells on mortality rates in the Dutch population. Environ. Health Perspect. 109, 463–470.

Kanti, F.S., Alari, A., Chaix, B., Benmarhnia, T., 2022. Comparison of various heat waves definitions and the burden of heat-related mortality in France: Implications for existing early warning systems. Environ. Res. 215 (Part 2), 114359.

Keikhosravi, Q., 2019. The effect of heat waves on the intensification of the heat island of Iran's metropolises (Tehran, Mashhad, Tabriz, Ahvaz). Urban Clim. 28, 100453.

Khandelwal, S., Goyal, R., Kaul, N., Mathew, A., 2017. Assessment of land surface temperature variation due to change in elevation of area surrounding Jaipur, India. Egypt. J. Remote Sens. Space Sci. 21, 1–8.

Kiarsi, M., Miresmaili, M., Mahmoodi, M.R., Farahmandnia, H., et al., 2023. Heat waves and adaptation: A global systematic review. J. Therm. Biol. 116, 103588.

Kılkış, Ş., 2022. Urban emissions and land use efficiency scenarios towards effective climate mitigation in urban systems. Renew. Sustain. Energy Rev. 167, 112733.

Kornus, A., Kornus, O., Klok, S., Danylchenko, O., Babenko, O., 2023. Heatwaves' characteristics detected by heat and cold wave index in Ukraine over the last four decades. Pol. J. Environ. Stud. 32 (4), 3175–3183.

Kotharkar, R., Bagade, A., 2018. Local climate zone classification for Indian cities: A case study of Nagpur. Urban Clim. 24, 369–392.

Kuttler, W., 2008. The urban climate – Basic and applied aspects. In: Marzluff, J.M., et al. (Eds.), Urban Ecology. Springer, Boston, MA. https://doi.org/10.1007/978-0-387-73412-5_13.

Lai, D., Liu, W., Gan, T., Liu, K., Chen, Q., 2019. A review of mitigating strategies to improve the thermal environment and thermal comfort in urban outdoor spaces. Sci. Total Environ. 661, 337–353.

Leichenko, R.M., Solecki, W.D., 2013. Climate change in suburbs: An exploration of key impacts and vulnerabilities. Urban Clim. 6, 82–97.

Li, L., Zha, Y., Wang, R., 2020. Relationship of surface urban heat island with air temperature and precipitation in global large cities. Ecol. Indic. 117, 106683.

Li, D., Wang, L., Liao, W., Sun, T., Katul, G., Zeid, E.B., Maronga, B., 2024. Persistent urban heat. Sci. Adv. 10, eadj7398.

Liao, J., Dai, Y., An, L., Hang, J., Shi, Y., Zeng, L., 2023. Water-energy-vegetation nexus explain global geographical variation in surface urban heat island intensity. Sci. Total Environ. 895, 165158.

Lokoshchenko, M.A., Alekseeva, L.I., 2023. Influence of meteorological parameters on the urban Heat Island in Moscow. Atmosphere 14, 507.
Ma, W., Jiang, G., Li, W., Zhou, T., 2018. How do population decline, urban sprawl and industrial transformation impact land use change in rural residential areas? A comparative regional analysis at the peri-urban interface. J. Clean. Prod. 205, 76–85.
Makvandi, M., Li, B., Elsadek, M., Khodabakhshi, Z., Ahmadi, M., 2019. The interactive impact of building diversity on the thermal balance and micro-climate change under the influence of rapid urbanization. Sustainability 11 (6), 1662.
Maleki Meresht, R., Sobhani, B., Moradi, M., 2021. Investigating the effect of heat waves on the intensification of heat islands in Sanandaj City from 1989 to 2018. Water Soil. 35 (5), 735–747.
Maleki Rashti, R., Sobhani, B., Moradi, M., 2022. Investigation of the relationship between heat waves and urban heat islands (case study: Ahvaz metropolis). Geogr. Dev. 20 (67), 121–141.
Mansouri Daneshvar, M., Rabbani, G., Shirvani, S., 2019. Assessment of urban sprawl effects on regional climate change using a hybrid model of factor analysis and analytical network process in the Mashhad city, Iran. Environ. Syst. Res. 8, 23.
Masson, V., Lemonsu, A., Hidalgo, J., Voogt, J., 2020. Annual review of environment and resources. Urban Clim. Clim. Chang. 45 (1), 411–444.
Miao, S., Zhan, W., Lai, J., Li, L., Du, H., Wang, C., Wang, C., Li, J., Huang, F., Liu, Z., Dong, P., 2022. Heat wave-induced augmentation of surface urban heat islands strongly regulated by rural background. Sustain. Cities Soc. 82, 103874.
Mihalakakou, G., Flocas, H.A., Santamouris, M., 2002. The impact of synoptic-scale atmospheric circulation on the urban heat island effect over Athens, Greece. In: 23rd AIVC and EPIC 2002 Conference (in Conjunction with 3rd European Conference on Energy Performance and Indoor Climate in Buildings) "Energy Efficient and Healthy Buildings in Sustainable Cities", Lyon, France.
Mika, J., Forgo, P., Lakatos, L., Olah, A.B., Rapi, S.R., Utasi, Z., 2018. Impact of 1.5K global warming on urban air pollution and heat island with outlook on human health effects. Curr. Opin. Environ. Sustain. 30, 151–159.
Mohan, M., Kikegawa, Y., Gurjar, B.R., 2013. Assessment of urban heat island effect for different land use–land cover from micrometeorological measurements and remote sensing data for megacity Delhi. Theor. Appl. Climatol. 112, 647–658.
Najah, F.T., Abdullah, S.F.K., Abdulkareem, T.A., 2023. Urban land use changes: effect of green urban spaces transformation on urban Heat Islands in Baghdad. Alex. Eng. J. 66, 555–571.
Nakano, H., Tanaka, R., Guan, S., Ohdan, H., 2023. Predicting rice grain yield using normalized difference vegetation index from UAV and GreenSeeker. Crop Environ. 2 (2), 59–65.
Nasiri, B., 2016. The investigation of summer heat waves in Tehran City. Mediterr. J. Soc. Sci. 7 (3 S2), 216.
Nobert, S., Pelling, M., 2017. What can adaptation to climate-related hazards tell us about the politics of time making? Exploring durations and temporal disjunctures through the 2013 London heat wave. Geoforum 85, 122–130.
Pande, C.B., Moharir, K.N., Varade, A.M., Mulla, G.A.S., Yaseen, Z.M., 2023. Intertwined impacts of urbanization and land cover change on urban climate and agriculture in Aurangabad city (MS), India using google earth engine platform. J. Clean. Prod. 422, 138541.
Peel, M.C., Finlayson, B.L., McMahon, T.A., 2007. "Updated World Map of the Koppen-Geiger Climate Classification" (PDF). hydrol-earth-syst-sci.net. University of Melbourne: Hydrology and Earth System Sciences, pp. 1633–1644. Retrieved May 8, 2017.
Półrolniczak, M., Kolendowicz, L., Majkowska, A., et al., 2017. The influence of atmospheric circulation on the intensity of urban heat island and urban cold island in Poznań, Poland. Theor. Appl. Climatol. 127, 611–625.
Rahaman, Z.A., Kafy, A.A., Saha, M., Rahim, A.A., Almulhim, A., Rahaman, S.N., Fattah, M.D., Rahman, M.T., et al., 2022. Assessing the impacts of vegetation cover loss on surface temperature, urban heat island and carbon emission in Penang city, Malaysia. Build. Environ. 222, 109335.
Reisi, M., Ahmadi Nadoushan, M., Aye, L., 2019. Remote sensing for urban heat and cool islands evaluation in semi-arid areas. Global J. Environ. Sci. Manage. 5 (3), 319–330.
Rendana, M., Idris, W.M.R., Rahim, S.A., 2023. Relationships between land use types and urban heat island intensity in Hulu Langat district, Selangor, Malaysia. Ecol. Process. 12, 33.
Roshan, Gh., Zanganeh Shahraki, S., Sauri, D., Borna, R., 2010. Urban sprawl and climatic changes in Tehran. J. Environ. Health Sci. Eng. 7 (1), 43–52.
Roshan, G.H., Ghanghermeh, A.A., Kong, Q., 2018. Spatial and temporal analysis of outdoor human thermal comfort during heat and cold waves in Iran. Weather Clim. Extrem. 19, 58–67.
Roshan, Gh.R., Sarli, R., Grab, S.W., 2021. The case of Tehran's urban heat island, Iran: Impacts of urban 'lockdown' associated with the COVID-19 pandemic. Sustain. Cities Soc. 75, 103263.
Roshan, Gh.R., Sarli, R., Fitchett, J.M., 2022. Urban heat island and thermal comfort of Esfahan City (Iran) during COVID-19 lockdown. J. Clean. Prod. 352, 131498.
Schwarz, N., Schlink, U., Franck, U., Großmann, K., 2012. Relationship of land surface and air temperatures and its implications for quantifying urban heat island indicators—An application for the city of Leipzig (Germany). Ecol. Indic. 18, 693–704.
Scott, A.A., Waugh, D.W., Zaitchik, B.F., 2018. Reduced urban Heat Island intensity under warmer conditions. Environ. Res. Lett. 13, 064003.
Semenzato, P., Bortolini, L., 2023. Urban Heat Island mitigation and urban green spaces: testing a model in the City of Padova (Italy). Land 12, 476.
Sharafkhani, R., Khanjani, N., Bakhtiari, B., Jahani, Y., Entezarmahdi, R., 2020. The effect of cold and heat waves on mortality in Urmia a cold region in the North West of Iran. J. Therm. Biol. 94, 102745.
Siddiqui, A., Kushwaha, G., Nikam, B., Srivastav, S.K., Shelar, A., Kumar, P., 2021. Analysing the day/night seasonal and annual changes and trends in land surface temperature and surface urban heat island intensity (SUHII) for Indian cities. Sustain. Cities Soc. 75, 103374.
Singh, S., Mall, R.K., 2023. Frequency dominates intensity of future heat waves over India. iScience 108263.
Stache, E., Schilperoort, B., Ottelé, M., Jonkers, H.M., 2022. Comparative analysis in thermal behaviour of common urban building materials and vegetation and consequences for urban heat island effect. Build. Environ. 213, 108489.
Stewart, L.D., Oke, T.R., 2012. Local climate zones for urban temperature studies. Bull. Am. Meteorol. Soc. 93 (12), 1879–1900.
Stewart, L.D., Oke, D.T.R., Scott Krayenhoff, E., 2014. Evaluation of the 'local climate zone' scheme using temperature observations and model simulations. Int. J. Climatol. 34, 1062–1080.
Tayyebi, A., Moghadam, H.S., Tayyebi, A.H., 2018. Analyzing long-term spatio-temporal patterns of land surface temperature in response to rapid urbanization in the mega-city of Tehran. Land Use Policy 71, 459–469.
Tol, Z., Ellis, A., 2023. Analysis of urban Heat Island intensity through air mass persistence: A case study of four United States cities. Urban Clim. 47, 101345.
Tsao, T.M., Hwang, J.S., Chen, C.Y., Lin, S.T., Tsai, M.J., Su, T.S., 2023. Urban climate and cardiovascular health: focused on seasonal variation of urban temperature, relative humidity, and PM2.5 air pollution. Ecotoxicol. Environ. Saf. 263 (115358).
Ullah, S., You, Q., Ullah, W., Sachindra, D.A., Ali, A., Bhatti, A.S., Ali, G., 2023. Climate change will exacerbate population exposure to future heat waves in the China-Pakistan economic corridor. Weather Clim. Extrem. 40, 100570.
Wang, Q., Wang, H., 2022. Spatiotemporal dynamics and evolution relationships between land-use/land cover change and landscape pattern in response to rapid urban sprawl process: a case study in Wuhan, China. Ecol. Eng. 182, 106716.
Wang, Y., Lin, L., Xu, Z., Wang, L., Huang, J., Li, G., Zhou, M., 2023. Have residents adapted to heat wave and cold spell in the 21st century? Evidence from 136 Chinese cities. Environ. Int. 173, 107811.
Wedler, M., Pinto, G.G., Hochman, A., 2023. More frequent, persistent, and deadly heat waves in the 21st century over the Eastern Mediterranean. Sci. Total Environ. 870, 161883.
Xu, Z., FitzGerald, G., Guo, Y., Jalaludin, B., Tong, S., 2016. Impact of heatwave on mortality under different heatwave definitions: a systematic review and meta-analysis. Environ. Int. 89–90, 193–203.
Yang, Y., Jin, C., Ali, S., 2020. Projection of heat wave in China under global warming targets of 1.5 °C and 2 °C by the ISIMIP models. Atmos. Res. 244, 105057.
Yang, S., Wang, L.L., Stathopoulos, T., Marey, A.M., 2023. Urban microclimate and its impact on built environment–a review. Build. Environ. 110334.
Yilmaz, S., Menteş, Y., Angin, S.N., Qaid, A., 2023. Impact of the COVID-19 outbreak on urban air, land surface temperature and air pollution in cold climate zones. Environ. Res. 237 (Part 2), 116887.

Yu, W., Zhou, W., 2018. Spatial pattern of urban change in two Chinese megaregions: contrasting responses to national policy and economic mode. Sci. Total Environ. 634, 1362–1371.
Yuan, S., Ren, Z., Shan, X., Deng, Q., Zhou, Z., 2023. Seasonal different effects of land cover on urban heat island in Wuhan's metropolitan area. Urban Clim. 49, 101547.
Zheng, Y., Li, W., Fang, C., Feng, B., Zhong, Q., Zhang, D., 2023. Investigating the impact of weather conditions on urban Heat Island development in the Subtropical City of Hong Kong. Atmosphere 14, 257.
Zhou, W., Yu, W., Zhang, Z., Cao, W., Wu, T., 2023. How can urban green spaces be planned to mitigate urban heat island effect under different climatic backgrounds? A threshold-based perspective. Sci. Total Environ. 890, 164422.